Applied Physics Letters

Direct imaging of fluorescence enhancement in the gap between two gold nanodisks

Cite as: Appl. Phys. Lett. **118**, 161105 (2021); https://doi.org/10.1063/5.0049395
Submitted: 04 March 2021 . Accepted: 07 April 2021 . Published Online: 20 April 2021

Hung-Ju Lin, Hengyang Xiang, Chenghao Xin, Zhelu Hu, Laurent Billot, Patrick Gredin, Michel Mortier, Zhuoying Chen, Maria-Ujué González, Antonio García-Martín, and Lionel Aigouy

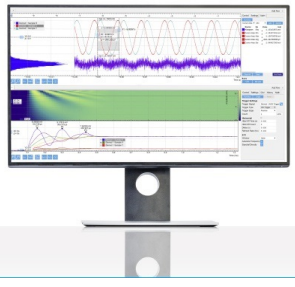

AIP Publishing

Applied Physics Letters ARTICLE scitation.org/journal/apl

Direct imaging of fluorescence enhancement in the gap between two gold nanodisks

Cite as: Appl. Phys. Lett. **118**, 161105 (2021); doi: 10.1063/5.0049395
Submitted: 4 March 2021 · Accepted: 7 April 2021 ·
Published Online: 20 April 2021

Hung-Ju Lin,[1] Hengyang Xiang,[1] Chenghao Xin,[1] Zhelu Hu,[1] Laurent Billot,[1] Patrick Gredin,[2,3] Michel Mortier,[2] Zhuoying Chen,[1] Maria-Ujué González,[4] Antonio García-Martín,[4] and Lionel Aigouy[1,a)]

AFFILIATIONS

[1]Laboratoire de Physique et d'Etude des Matériaux (LPEM), CNRS, ESPCI Paris, PSL Research University, Sorbonne Université, 10 rue Vauquelin, F-75231 Paris, France
[2]Institut de Recherche de Chimie Paris, Chimie ParisTech, CNRS, PSL Research University, 11 rue Pierre et Marie Curie, F-75005 Paris, France
[3]Sorbonne Université, Faculté des sciences en Ingénierie, 4 place Jussieu, F-75005 Paris, France
[4]Instituto de Micro y Nanotecnología IMN-CNM, CSIC, CEI UAM+CSIC, Isaac Newton 8, E-28760 Tres Cantos, Madrid, Spain

[a)]**Author to whom correspondence should be addressed:** lionel.aigouy@espci.fr

ABSTRACT

We present an analysis of the optical coupling between two gold nanodisks by near-field fluorescence microscopy. This is achieved by simultaneously scanning and measuring the light emitted by a single Er^{3+}/Yb^{3+} doped nanocrystal glued at the end of an atomic force microscope tip. The excitation of the nanocrystal was performed at $\lambda = 975$ nm via upconversion, and fluorescence was detected in the visible part of the spectrum at $\lambda = 550$ nm. For an isolated nanodisk, the near-field presents a two-lobe pattern oriented along the direction of the incident polarization. For two nanodisks with a sizable separation distance (385 nm) illuminated with the polarization along the interparticle axis, we observe a negative effect of the coupling with a slight decrease in fluorescence in the gap. For smaller gap values (195, 95, and 55 nm), a strong increase in fluorescence is observed as well as a reduced spatial localization of the field as the distance decreases. Finally, when the disks touch each other (0 nm), the dipolar–dipolar interaction between them disappears and no fluorescence enhancement occurs. A new plasmon mode is created at another wavelength. Our experimental results are in good agreement with numerical simulations of the near-field intensity distribution at the excitation wavelength on the surface of the structures. Combining fluorescence mapping and far-field scattering spectroscopy should be of strong interest to develop bio-chemical sensors based on field enhancement effects.

Metallic nanostructures made of gold and silver exhibit extraordinary properties due to the presence of surface plasmon resonances (SPRs).[1–4] These resonances are due to the collective oscillation of electrons on the metal surface and are characterized by a strong absorption and scattering of light. At the local scale, they induce a localization of the electromagnetic field at some specific locations around the nanostructures as well as strong enhancements of the intensity. Numerous applications arise from this field enhancement effect in different domains such as increasing the detection sensitivity for biosensing,[3,5–7] surface enhanced Raman scattering (SERS),[8,9] or improving the performance of optoelectronic devices.[10–12] The intensity of the local fields depends on the nature of the metallic nanoparticles, their shape and size, and the dielectric environment. Groups of nanoparticles can also lead to an even larger increase in the field enhancement due to the coupling between them. In the case of metallic dimers, if the separation distance is small enough, near-field interaction occurs between them and this leads to a strongly enhanced and localized electromagnetic field.[13–18] If the molecules are inserted in the gap, the emission can be enhanced,[19,20] either by an increase in the excitation or by an increase in the fluorescence decay rate or by both effects.[21–27]

To observe the coupling effects between two metallic dimers, a widely used method is far-field scattering or transmission spectroscopy on isolated dimers or on structures arranged in arrays.[13,16,17,28–30] The scattering spectra of two coupled nanoparticles exhibit a red shift of the dipolar resonance compared to the isolated ones. This can be understood by the fact that if we approach two dipoles, i.e., the two nanostructures, the resonance frequency varies due to the dipole–dipole interaction. Other techniques like scattering scanning near-field optical microscopy (SNOM)[31,32] and electron energy loss spectroscopy

(EELS) as well as tomographic EELS mapping[33,34] directly showed the light localization in the gap between nanostructures with a lateral resolution that can be as small as 10 nm. Finally, non-linear far-field imaging techniques like second harmonic generation also evidenced the coupling of plasmons between two nanostructures.[35,36] The intensity of the coupling depends on the distance between the nanostructures. For instance, red shifts of the resonance can be detected if the gap is smaller than approximately 2.5 times the particle diameter.[13] In the case of a nanodisk of 200 nm diameter, this corresponds to a gap of 500 nm. When the distance becomes very small, the electromagnetic field localization and enhancement become very high due to the accumulation of charges in the gap, but they start to vanish at very short distances ($d < 1$ nm), for which the dipolar resonance is inhibited. Finally, when the particles touch each other ($d = 0$ nm), a new nanostructure is created with other resonances, and new scattering peaks appear at other wavelengths in the near-infrared.[15,28]

In this article, our aim is to explore how the coupling between two gold nanodisks influences the fluorescence emitted by a single nanocrystal. This will be achieved by mapping the fluorescence intensity as a function of the position of the nanocrystal around the disks, for different separation distances between them. Although there are many experimental studies describing the influence of plasmonic structures on fluorescent molecules,[19–27,37] the direct mapping of the emission intensity or lifetime has only been achieved on simple structures like isolated metallic nanostructures.[23,38] For structures where coupling effects or interactions govern the optical response, many questions are still unanswered. How does the nanocrystal fluorescence evolve as a function of the gap length? How is the fluorescence intensity related to the near-field intensity at the excitation wavelength? Do we observe a total quenching of fluorescence when two coupled structures touch each other? To perform the aforementioned fluorescence mapping, so that we can shed some light on these questions, we use a fluorescent nanocrystal glued at the end of an atomic force microscope (AFM) tip and measure the emitted light as a function of the tip position around the nanostructures.

To be able to perform quantitative comparisons on a series of coupled nanodisks, it is required to use the same tip/nanocrystal for all the samples. Therefore, the nanocrystal has to be robust, durable, and should not present any evidence of photobleaching. Fluoride nanocrystals doped with Er^{3+} and Yb^{3+} ions nicely satisfy these conditions.[38–41] In this study, we use $NaYF_4$:Er^{3+}/Yb^{3+} nanocrystals synthesized by the hydrothermal route.[42,43] Some details about the synthesis can be found in the supplementary material. Er^{3+}/Yb^{3+} co-doped materials emit fluorescence at the green ($\lambda = 525$ nm), the yellowish-green ($\lambda = 550$ nm), and the red ($\lambda = 670$ nm) wavelengths in the visible region of the electromagnetic spectrum. It is possible to excite them in the visible with a one-photon excitation and also in the near-infrared by upconversion, for instance at $\lambda = 975$ nm. This two-photon process is very convenient because the excitation wavelength is well separated from the emission lines and it is easy to get rid of the incident light.

We show in Fig. 1 the experimental setup, a scanning electron microscope (SEM) image of the nanocrystals, their energy band diagram, and their fluorescence spectrum. The sample is excited in a transmission mode with a linearly polarized, intensity modulated ($f = 330$ Hz), laser diode emitting at $\lambda_{EXC} = 975$ nm. The beam is focused on a 20 μm wide spot and that illuminates both the sample

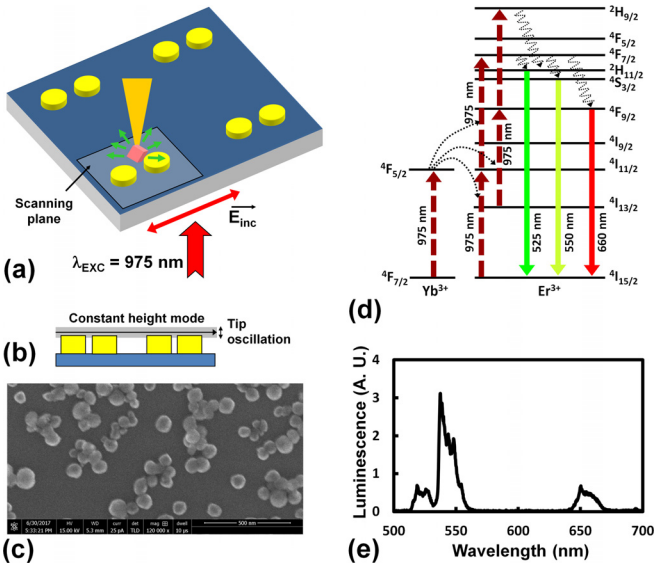

FIG. 1. Sketch of the illumination configuration (a) and the scanning mode (b), SEM image of a 100–150 nm large fluorescent $NaYF_4$:Er^{3+}/Yb^{3+} nanocrystals (c), energy band diagram (d), and luminescence spectrum of the nanocrystals. The excitation was performed at $\lambda_{EXC} = 975$ nm.

surface and the nanocrystal. The emitted light ($\lambda = 550$ nm) is collected with a high numerical aperture objective and sent to a photomultiplier tube and a lock-in amplifier synchronized to the laser modulation. The scans are performed in the tapping mode, with the feedback loop disabled, at a constant height ($h = 0$ nm) above the nanostructures [see Fig. 1(b)]. Before studying coupled nanostructures, we measured the fluorescence intensity maps near an isolated gold nanodisk fabricated by electron beam lithography on a glass substrate. The diameter and the thickness of the disk were close to 240 and 50 nm, respectively. The results are shown in Fig. 2, where the fluorescence maps are composed of two high intensity zones, which form two lobes oriented in the direction of the incident polarization of the excitation beam. As shown in Figs. 2(a) and 2(b), when the polarization is rotated by 90°, the lobes also rotate by the same angle. Recently, a complete study on similar structures showed that the fluorescence maps are directly linked to the near-field intensity near the nanostructure at the excitation wavelength.[38] It was observed that the maximum fluorescence occurred for disk diameters in the 200–250 nm range and a good agreement was found with numerical simulations.

To put forward the role of interactions, we now consider the case of two almost identical nanodisks, where the near-field intensity and the nanocrystal fluorescence depend on the coupling and on the disk separation distance. We characterized five structures of diameter 240 nm and separated, from edge to edge, by $d = 385$, 195, 95, 55, and 0 nm, respectively. The chosen diameter for each disk corresponds to that which has the largest local electromagnetic field intensity at the excitation wavelength[38] and the separation distances cover a wide range, from mid-field, where we expect a reduced (but not vanishing) influence of evanescent coupling, to near-field coupling and direct contact. The polarization of the incident light is parallel to the alignment of two nanodisks. In all the experiments, we used the same tip/

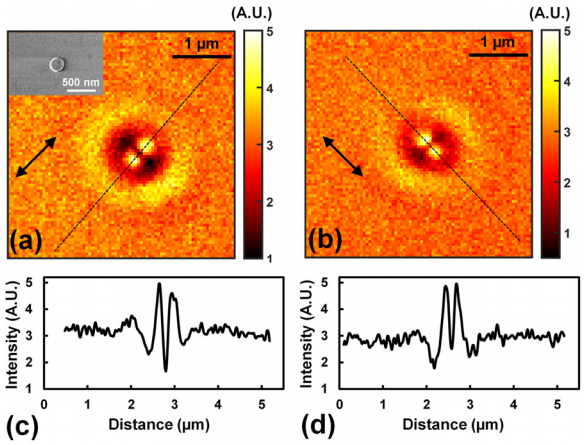

FIG. 2. Near-field fluorescence maps (a) and (b) and cross sections (c) and (d) measured when a nanocrystal is scanning an isolated 240 nm-large gold nanodisk. The excitation was performed at $\lambda_{EXC} = 975$ nm, and the luminescence was detected in the 520–550 nm range. The incident polarization of the laser beam is indicated by the arrow. The inset is an SEM picture of the nanodisk.

nanocrystal, performing the measurements in nearly identical experimental conditions.

Let us start with the largest separation distance $d = 385$ nm, whose experimental fluorescence image and a cross section are shown in Figs. 3(a) and 3(b), respectively. Even for a large gap, we can see that the fluorescence pattern is not simply the addition of the contribution of two isolated nanodisks. There are four lobes, aligned in the same direction, but the lobes situated in the gap are less intense than the external ones [see Figs. 3(a) and 3(b)]. This shows that, even for this large distance, there is a measurable interaction and the presence of one disk modifies the near-field around the other. This observation

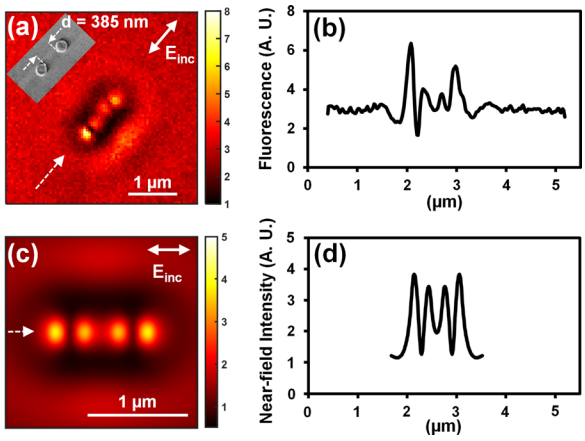

FIG. 3. Experimental fluorescence image (a) and cross section (b) measured on coupled gold nanodisks with a separation distance $d = 385$ nm. FDTD simulation (c) and (d) of the electromagnetic field intensity at the excitation wavelength. The intensity is averaged over a 100 nm large cube and in a plane situated 14 nm above the nanodisk surface. The cross sections are extracted from the images in the direction indicated by the white dashed arrow. The incident polarization is parallel to the alignment of the disks. The inset is an SEM picture of the disks.

agrees with the measurements performed by Su *et al.*[13] and Hooshmand and El-Sayed[18] who observed that the red shift of the resonance due to the coupling between two nanoparticles could be observed when the gap distance is up to 2.5 times larger than the diameter of the particles (in our case, the ratio gap/diameter is 1.6 times smaller than this value). For comparison, we performed rigorous electromagnetic calculations using the finite difference time domain (FDTD) method to obtain the spatial distribution of the near-field intensity ($||E||^2$) above the disk dimer. To account for the finite fluorescent particle size, the intensity is averaged on a 100^3 nm^3 large cube. The "cube" is scanned in a plane above the disk surface at a constant height of 14 nm. The near-field intensity map and a cross sectional profile along the alignment are shown in Figs. 3(c) and 3(d), respectively. As for the experimental fluorescence maps, four lobes are clearly discernible, oriented along the direction of the incident polarization, the ones located in the gap between the disks being less intense than the external ones. This qualitatively agrees with the experimental results; however, the relative intensity of the inner lobes compared to that of the outer ones is slightly smaller in the fluorescence map than in the simulation. The difference can be explained by several reasons. To simplify the simulation, the average was made on a cube that does not exactly represent the real shape of the nanocrystal; its shape is more or less spherical (see the SEM image in Fig. 1). Also, the nanocrystal is not a pure detector of the electromagnetic field. It is also a light source excited by the near-field, and the emission process (for instance, the radiative rate and the emission pattern) can also be influenced by the gold dimer. These effects are not considered in the simulation and would be way too hard to implement. Despite the mentioned differences, the agreement is good enough to consider that the physical role played by the interaction is well captured for this separation distance.

In Fig. 4, we show both the experimental fluorescence maps and profiles measured on dimers having a smaller gap (larger interaction) and the corresponding FDTD numerical results. As the gap reduces to $d = 195$ nm, the inner lobes combine with each other and the resulting intensity becomes larger than that of the external lobes [Fig. 4(a)]. This is quite the opposite behavior observed for $d = 385$ nm. Once more, the simulation [Fig. 4(c)] agrees well with the experimental image. When the distance decreases to $d = 95$ nm, the central lobe becomes yet more intense and then the intensity slightly decreases for $d = 55$ nm. This effect is illustrated in Fig. 4(m), where we plotted the evolution of fluorescence of the central lobe, normalized both by the fluorescence far from the dimer and by the lobe fluorescence of the 385 nm structure. The first normalization allows us to get rid of intensity variations when we move the tip from one structure to the others. The second normalization allows us to directly compare the evolution of the lobe intensity with numerical simulations. The normalized near-field intensity of the central lobe deduced from the simulations is also shown, in good agreement with the experiment. For $d < 195$ nm, we can see that the relative fluorescence is larger than that of an isolated disk of the same dimensions, represented by the horizontal green line in Fig. 4(m). This clearly shows that the association of two particles increases the local enhancement effects compared to a single structure but it also shows that there is a maximum fluorescence intensity observed for $d = 95$ nm. It is perhaps relevant to recall that the fluorescence experimentally obtained corresponds to an average over the whole of the volume of the fluorescent nanocrystal above the

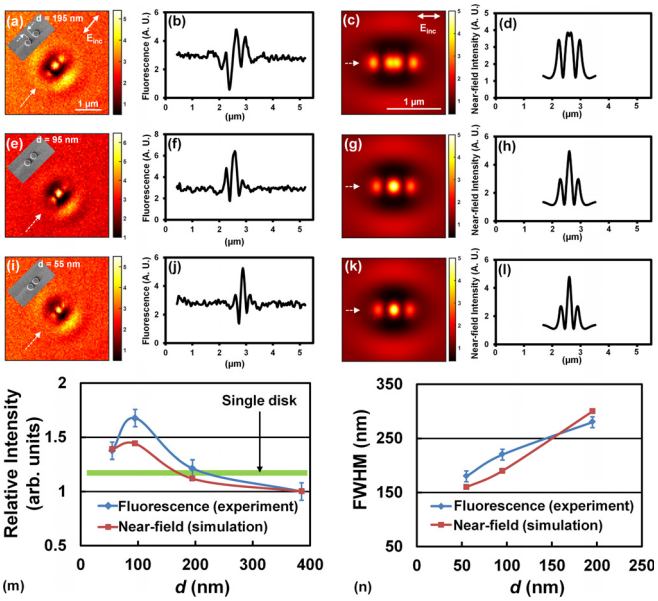

FIG. 4. Experimental fluorescence maps (a), (e), and (i) and cross sectional profiles (b), (f), and (j) measured on coupled gold dimers with various separation distances. FDTD simulations (c), (g), and (k) and cross sections (d), (h), and (l) of the electromagnetic field intensity at the excitation wavelength. The separation distance between the dimers is 195 nm (a)–(d), 95 nm (e)–(h), 55 nm (i)–(l). The cross sections are taken along the dashed arrows. The insets in (a), (e), and (i) are SEM images of the gold dimers. Experimental fluorescence and calculated near-field relative intensities of the central lobe as a function of the separation distance d (m). The intensities are normalized by the intensities far from the dimers and also by the value for $d = 385$ nm (reference value). FWHM of the central lobe as a function of the separation distance d (n). In (m), the horizontal green line represents the fluorescence intensity of the lobes for an isolated single disk, extracted from Fig. 2.

dimers at an average height of 55 nm. It is likely that reducing the integration volume and scanning the surface closer to the gap would give a maximum value for a smaller separation distance. Indeed, in the gap itself, very large enhancements have been calculated for gaps smaller than 5 nm.[14,18,44–47] We are not sensitive to these strong fields here because our tip/nanocrystal is not able to penetrate inside the gap due to its size. Reducing the gap has also an effect on the full width at half maximum (FWHM) of the central fluorescence lobe. As we can see in Fig. 4(n), as the gap reduces from 195 to 55 nm, the FWHM decreases by almost a factor of 2 for both the fluorescence and the simulation. This evidences the stronger localization of the electromagnetic field for small separation distances.

The interaction between the gold disks is more complex when they are very close to each other, and higher order modes can appear at lower wavelengths if d becomes smaller than 1 nm (Refs. 15, 18, and 48) as the electronic cloud influences the dielectric properties of the gap, in a very similar way to the finite size corrections in atomic size conductors back in the 1990s.[49] Although the local electromagnetic field is very high in the gap for these distances, quantum mechanical effects like electron tunneling can also lead to a decrease in the local enhancement at distances smaller than 0.5 nm.[50] We are not sensitive to these effects with our tip and nanocrystal, but we observed that when the disks contact each other, we do not observe any fluorescence enhancement. This is clearly evident on the fluorescence image and cross section shown in Fig. 5, where the central lobe disappears and the external ones are barely noticeable. The experiment is, once more, corroborated by our FDTD numerical simulation, which shows the very same intensity reduction on the whole structure. A small increase remains observable in the middle of the dark zone (see the cross sections in Fig. 5), but it apparently comes from the lateral parts of the dimer.

The fluorescence (and near-field) map for the touching dimer actually resembles that of a "big" lone disk,[38] and, thus, we can explain the disappearance of the fluorescence bright spot as caused by the presence of the conductive path between the two disks. Electrons do not oscillate anymore around each disk separately; they can go back and forth between the two disks, which shifts the resonance frequency of the system at another, larger, wavelength, far from the excitation source.[28,50] Therefore, the associated near-field and fluorescence enhancements do not occur anymore. The experiments described here were performed with the incident polarization aligned along the dimer long axis. We also performed experiments with the incident polarization perpendicular to the interparticle axis (see the supplementary material). In that case, the two disks behave like isolated structures, with the two lobes positioned on each side of the disks, and the experiments do not exhibit any evidence of coupling between the disks.

In summary, we performed the direct mapping of fluorescence enhancement effects between two coupled gold nanodisks. All the experiments were compared to the intensity of the near-field distribution at the excitation wavelength calculated by FDTD. A very good agreement is observed which shows that, for the kind of nanocrystal we used, fluorescence emission is well described by absorption effects. We characterized the transition from well-separated to touching disks. We first showed that even for a large separation distance (385 nm), the fluorescence between two disks is modified compared to isolated structures, and the central lobe is quenched compared to the external one. Then, for smaller separation distances, the fluorescence at central lobes is strongly increased due to the evanescent coupling between the disks. As the disks touch each other, fluorescence is almost totally quenched

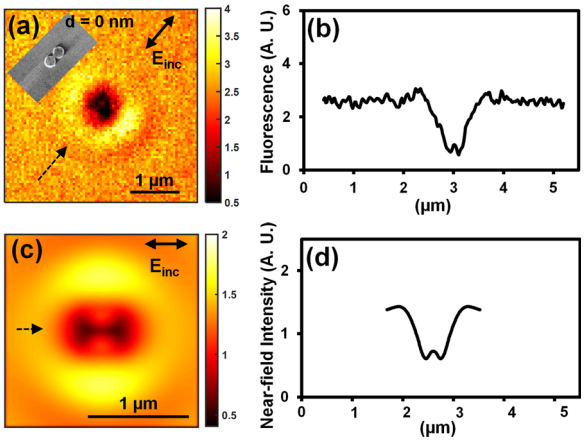

FIG. 5. Experimental fluorescence image (a) and cross section (b) measured on a structure with touching nanodisks ($d = 0$ nm); FDTD simulation (c) and cross section (d) of the electromagnetic field intensity on the structure. The inset in (a) is an SEM image of the dimer.

due to the suppression of the dipole–dipole coupling and the appearance of another plasmon mode at larger wavelengths, as if the dimer were a bigger disk. Combined with far-field extinction or absorption spectroscopy, we think that the direct visualization of fluorescence maps near nanostructures can be very interesting to design and optimize sensors based on local field enhancement effects.

See the supplementary material for the fabrication of fluorescent nanoparticles, the tip fabrication procedure, and additional near-field fluorescence experiments.

The authors thank the support from the DIM Nano-K program from "Région Ile de France," from the Idex Paris Sciences & Lettres through Grant No. ANR-10-IDEX-0001-02 PSL from the CNRS and the CSIC through the Spanish-French program PICS (Grant Nos. SolarNano PICS07687 and PIC2016FR2), and from the Spanish Ministerio de Ciencia e Innovación through Grant No. PID2019-109905GA-C22.

DATA AVAILABILITY

The data that support the findings of this study are available from the corresponding author upon reasonable request.

REFERENCES

[1]S. A. Maier, *Plasmonics: Fundamentals and Applications* (Springer Verlag, 2007), pp. 65–88.
[2]J. A. Schuller, E. S. Barnard, W. Cai, Y. C. Jun, J. S. White, and M. L. Brongersma, Nat. Mater. **9**, 193 (2010).
[3]K. M. Mayer and J. H. Hafner, Chem. Rev. **111**, 3828 (2011).
[4]N. Jiang, X. Zhuo, and J. Wang, Chem. Rev. **118**, 3054 (2018).
[5]K. A. Willets and R. P. Van Duyne, Annu. Rev. Phys. Chem. **58**, 267 (2007).
[6]P. Offermans, M. C. Schaafsma, S. R. K. Rodriguez, Y. Zhang, M. Crego-Calama, S. H. Brongersma, and J. G. Rivas, ACS Nano **5**, 5151 (2011).
[7]K. Saha, S. S. Agasti, C. Kim, X. Li, and V. M. Rotello, Chem. Rev. **112**, 2739 (2012).
[8]C. L. Haynes, A. D. McFarland, and R. P. V. Duyne, Anal. Chem. **77**, 338A (2005).
[9]C. Zong, M. Xu, L.-J. Xu, T. Wei, X. Ma, X.-S. Zheng, R. Hu, and B. Ren, Chem. Rev. **118**, 4946 (2018).
[10]K. Ueno, T. Oshikiri, Q. Sun, X. Shi, and H. Misawa, Chem. Rev. **118**, 2955 (2018).
[11]H. A. Atwater and A. Polman, Nat. Mater. **9**, 205 (2010).
[12]C. Y. Cho, S. J. Lee, J. H. Song, S. H. Hong, S. M. Lee, Y. H. Cho, and S. J. Park, Appl. Phys. Lett. **98**, 051106 (2011).
[13]K.-H. Su, Q.-H. Wei, X. Zhang, J. J. Mock, D. R. Smith, and S. Schultz, Nano Lett. **3**, 1087 (2003).
[14]E. Hao and G. C. Schatz, J. Chem. Phys. **120**, 357 (2004).
[15]I. Romero, J. Aizpurua, G. W. Bryant, and F. J. García de Abajo, Opt. Express **14**, 9988 (2006).
[16]S. Sheikholeslami, Y. W. Jun, P. K. Jain, and A. P. Alivisatos, Nano Lett. **10**, 2655 (2010).
[17]N. J. Halas, S. Lal, W.-S. Chang, S. Link, and P. Nordlander, Chem. Rev. **111**, 3913 (2011).
[18]N. Hooshmand and M. A. El-Sayed, Proc. Natl. Acad. Sci. **116**, 19299 (2019).
[19]M. Chekini, R. Filter, J. Bierwagen, A. Cunningham, C. Rockstuhl, and T. Bürgi, J. Appl. Phys. **118**, 233107 (2015).
[20]A. P. Francisco, D. Botequim, D. M. F. Prazeres, V. V. Serra, S. M. B. Costa, C. A. T. Laia, and P. M. R. Paulo, J. Phys. Chem. Lett. **10**, 1542 (2019).
[21]P. Anger, P. Bharadwaj, and L. Novotny, Phys. Rev. Lett. **96**, 113003 (2006).
[22]S. Kühn, U. Håkanson, L. Rogobete, and V. Sandoghdar, Phys. Rev. Lett. **97**, 017402 (2006).
[23]D. Cao, A. Cazé, M. Calabrese, R. Pierrat, N. Bardou, S. Collin, R. Carminati, V. Krachmalnicoff, and Y. De Wilde, ACS Photonics **2**, 189 (2015).
[24]G. P. Acuna, M. Bucher, I. H. Stein, C. Steinhauer, A. Kuzyk, P. Holzmeister, R. Schreiber, A. Moroz, F. D. Stefani, T. Liedl, F. C. Simmel, and P. Tinnefeld, ACS Nano **6**, 3189 (2012).
[25]G. Schneider, G. Decher, N. Nerambourg, R. Praho, M. H. V. Werts, and M. Blanchard-Desce, Nano Lett. **6**, 530 (2006).
[26]V. Flauraud, R. Regmi, P. M. Winkler, D. T. L. Alexander, H. Rigneault, N. F. van Hulst, M. F. Garcia-Parajo, J. Wenger, and J. Brugger, Nano Lett. **17**, 1703 (2017).
[27]J. T. Hugall, A. Singh, and N. F. van Hulst, ACS Photonics **5**, 43 (2018).
[28]T. Atay, J.-H. Song, and A. V. Nurmikko, Nano Lett. **4**, 1627 (2004).
[29]W. Zhang, Q. Li, and M. Qiu, Opt. Express **21**, 172 (2013).
[30]O. L. Muskens, V. Giannini, J. A. Sanchez-Gil, and J. Gómez Rivas, Opt. Express **15**, 17736 (2007).
[31]M. Schnell, A. Garcia-Etxarri, J. Alkorta, J. Aizpurua, and R. Hillenbrand, Nano Lett. **10**, 3524 (2010).
[32]P. Alonso-González, P. Albella, F. Golmar, L. Arzubiaga, F. Casanova, L. E. Hueso, J. Aizpurua, and R. Hillenbrand, Opt. Express **21**, 1270 (2013).
[33]S. Kadkhodazadeh, J. Rosenkrantz de Lasson, M. Beleggia, H. Kneipp, J. Birkedal Wagner, and K. Kneipp, J. Phys. Chem. C **118**, 5478 (2014).
[34]G. Haberfehlner, A. Trügler, F. P. Schmidt, A. Hörl, F. Hofer, U. Hohenester, and G. Kothleitner, Nano Lett. **15**, 7726 (2015).
[35]A. Slablab, L. Le Xuan, M. Zielinski, Y. de Wilde, V. Jacques, D. Chauvat, and J.-F. Roch, Opt. Express **20**, 220 (2012).
[36]J. Berthelot, G. Bachelier, M. Song, P. Rai, G. Colas des Francs, A. Dereux, and A. Bouhelier, Opt. Express **20**, 10498 (2012).
[37]A. F. Koenderink, ACS Photonics **4**, 710 (2017).
[38]L. Aigouy, M.-U. González, H.-J. Lin, M. Schoenauer-Sebag, L. Billot, P. Gredin, M. Mortier, Z. Chen, and A. García-Martín, Nanoscale **11**, 10365 (2019).
[39]S. Schietinger, T. Aichele, H.-Q. Wang, T. Nann, and O. Benson, Nano Lett. **10**, 134 (2010).
[40]D. Lu, S. K. Cho, S. Ahn, L. Brun, C. J. Summers, and W. Park, ACS Nano **8**, 7780 (2014).
[41]H.-J. Lin, K. de Oliveira Lima, P. Gredin, M. Mortier, L. Billot, Z. Chen, and L. Aigouy, Appl. Phys. Lett. **111**, 251109 (2017).
[42]J. Zhao, Y. Sun, X. Kong, L. Tian, Y. Wang, L. Tu, J. Zhao, and H. Zhang, J. Phys. Chem. B **112**, 15666 (2008).
[43]H. Xiang, Z. Hu, L. Billot, L. Aigouy, W. Zhang, I. McCulloch, and Z. Chen, ACS Appl. Mater. Interfaces **11**, 42571 (2019).
[44]A. Gopinath, S. V. Boriskina, W. R. Premasiri, L. Ziegler, B. M. Reinhard, and L. Dal Negro, Nano Lett. **9**, 3922 (2009).
[45]O. Lecarme, T. Pinedo-Rivera, K. Berton, J. Berthier, and D. Peyrade, Appl. Phys. Lett. **98**, 083122 (2011).
[46]S. K. Pal, H. Chatterjee, and S. K. Ghosh, RSC Adv. **9**, 42145 (2019).
[47]A. García-Martín, D. R. Ward, D. Natelson, and J. C. Cuevas, Phys. Rev. B **83**, 193404 (2011).
[48]J. B. Lassiter, J. Aizpurua, L. I. Hernandez, D. W. Brandl, I. Romero, S. Lal, J. H. Hafner, P. Nordlander, and N. J. Halas, Nano Lett. **8**, 1212 (2008).
[49]A. Garcia-Martin, J. A. Torres, and J. J. Saenz, Phys. Rev. B **54**, 13448 (1996).
[50]J. Zuloaga, E. Prodan, and P. Nordlander, Nano Lett. **9**, 887 (2009).